Available online at www.sciencedirect.com
SCIENCE DIRECT®
Atmospheric Environment 39 (2005) 6194–6203
ATMOSPHERIC ENVIRONMENT
www.elsevier.com/locate/atmosenv

The Washington aerial spray drift study: Modeling pesticide spray drift deposition from an aerial application

Ming-Yi Tsai[a,*], Kai Elgethun[a,c], Jaya Ramaprasad[a], Michael G. Yost[a], Allan S. Felsot[b], Vincent R. Hebert[b], Richard A. Fenske[a]

[a]*Department of Environmental & Occupational Health Sciences, University of Washington, Seattle, WA 98195, USA*
[b]*Food and Environmental Quality Laboratory, Washington State University, Richland, WA 99352, USA*
[c]*Department of Geography, Texas A&M University, College Station, TX 77843, USA*

Received 15 March 2005; accepted 1 July 2005

Abstract

A routinely scheduled aerial organophosphorus pesticide application of methamidophos in central Washington State was monitored in the summer of 2002. The sprayed potato crop surrounded a rural agricultural community where residences were within 200 meters of the sprayed fields. Modeling pesticide spray drift is critical for exposure assessment of the residential population. Herein the objective is to model spray drift deposition with regard to model selection, calibration, and prediction for a particular application event. The US Environmental Protection Agency's Fugitive Dust Model (FDM) was chosen for its flexibility in terms of both inputs and outputs. Model calibration was accomplished by varying the aerosol size distribution in comparison with collected deposition samples and locating the minimum relative bias measure. From the calibrated model, a map of total pesticide deposition within the community indicated spray drift occurring despite adherence to general precautionary pesticide application guidelines. The calibrated model also provided 15-min time-resolved deposition images over the 5-h application period. These time-resolved maps revealed that actual community deposition occurred in only 2 of the 20 time periods when the source, due to the changing wind, was oriented towards the community. Despite the limitations of FDM in modeling a liquid aerosol, the calibration of the model to samplers located in the areas of interest allows it to serve as a potential tool for conducting exposure assessment within the community.
© 2005 Elsevier Ltd. All rights reserved.

Keywords: FDM; Gaussian dispersion; Deposition sampling; Pesticide aerosol

1. Introduction

Despite general guidelines for minimizing pesticide spray drift during application, pesticide spray drift continues to be a concern in rural agricultural communities. Most studies of pesticide spray drift have focused on the extent of near-field drift under varying meteorology by application method (Fox et al., 1990, 1993; Ganzelmeier et al., 1995; MacCollom et al., 1985; MacNeil and Hikichi, 1986; Salyani and Cromwell, 1992). At the same time, most human pesticide exposure assessment studies have conducted monitoring of pesticide levels in backyards, inside houses from carpets and surfaces and through biomonitoring of human subjects without modeling the source of the spray event(s) of concern (Fenske et al., 2002; Garcia et al., 2000; Koch et al., 2002; Lu et al., 2000; Richards et al.,

*Corresponding author. Tel.: +1 206 685 3250.
E-mail address: mytsai@u.washington.edu (M.-Y. Tsai).

1352-2310/$ - see front matter © 2005 Elsevier Ltd. All rights reserved.
doi:10.1016/j.atmosenv.2005.07.011

2001). Both approaches have yielded insight into, respectively: (1) the extent and characteristics of off-target drift depending on the meteorological factors, application method, and pesticide composition; and (2) the levels of pesticide residues that can be found in and around rural agricultural residences. Only a few studies have focused on assessing human exposure to spray drift from specific pesticide applications (Ames et al., 1993; Shehata et al., 1984).

Currently, general spray drift reduction guidelines are specified in the pesticide labels by application type. The following are recommendations for aerial applications: (a) no application within 150 feet (46 m) of an unprotected person or occupied dwelling; (b) use largest droplet size consistent with acceptable pest control; (c) spray when wind speeds are between 3 and 10 mph (1.3 and 4.5 m s^{-1}); (d) do not spray when winds are above 15 mph (6.7 m s^{-1}); (e) avoid spraying in low humidity and high temperature conditions; (f) do not spray during temperature inversions. (For greater detail see *Monitor 4* pesticide label (Valent, 2001)). Although these general guidelines are sound and reasonable, their limitations are attested to by the continued concern over spray drift.

Pesticide drift modeling is capable of resolving the difficulties of determining exposure to community residents and bystanders. Estimating exposure during and after spray operations is difficult because of the large area of concern and the interspersing of housing with farmland. Traditional air and deposition sampling of such a large area would be prohibitively expensive. Furthermore, such methods often do not provide finely time-resolved data but are instead integrated over relatively long sampling periods. The long sampling period, on the order of hours for many methods, in relation to the relatively short spray event (an hour for an 85 acre (34.4 ha) crop circle) does not allow the investigator to understand the evolution of any spray event. Therefore, modeling is an essential component for estimating the spread, deposition concentration, and time evolution of spray drift. The objective of this paper is to model the ground deposition component of drift. A companion paper examines gas phase concentrations due to post-spray volatilization of the pesticide from wetted fields (Ramaprasad et al., 2004).

2. Methods

2.1. Background

An extensive children's exposure assessment study was conducted in July of 2002 during scheduled pesticide applications (Elgethun, 2004; Weppner et al., 2005). Modeling of spray drift was an essential component of this exposure assessment study. This monitoring experiment was conducted in a rural agricultural area in central Washington State where five potato crop circles were aerially sprayed with *Monitor 4* (Valent, 2001) whose active ingredient is methamidophos (O,S-dimethyl phosphoramidothioate). Methamidophos is an organophosphate pesticide used to protect the crop against aphids and thrips. The five crop circles surround a community that houses many local farm workers and their families (Fig. 1). All residences were located within 800 m of each other and each residence was located within 15–200 m of the nearest sprayed field. Along with air concentration measures, pesticide deposition samples were collected in 22 locations.

Modeling was necessary for several reasons: (1) the limited number of actual samplers; (2) the lack of time resolution in actual sampling methods; and (3) multiple exposure pathways. As can be imagined, the possible spatial locations of the children far exceeded the number of samplers that could be feasibly deployed. Furthermore, pesticide residue sampling cards were laid out over relatively long periods of time, thereby providing little if any time resolution. A drift model, calibrated with existing sampling data, allowed us to predict cumulative pesticide loadings in locations where no sampling data were available. Additionally, the model provided time-resolved surface loading data according to the resolution of the available meteorological data. Ultimately, by modeling both surface deposition and air concentration and incorporating these results into an exposure assessment study, we can begin to differentiate the contribution of the three exposure pathways of

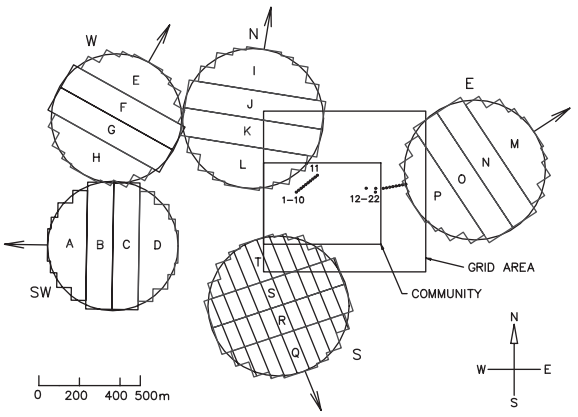

Fig. 1. Map of community and surrounding fields. The deposition samplers are numbered 1–22 and are indicated by the small dots within the grid area (800 × 800 m). The community area is indicated by the smaller rectangle within the grid area. There are five potato crop circles: SW, W, N, E, and S. The arrows indicate the initial 15-min wind direction when spraying began on that particular field. The letters A–T represent 15-min swaths that were laid by the plane. The hashed crop circle was sprayed in the afternoon.

aerosol inhalation, skin/surface transfer, and gas phase inhalation.

2.2. Aerial application notes

The potato crop was sprayed by a fixed-wing aircraft with methamidophos insecticide (*Monitor 4*) at a rate of 1 pound active ingredient per acre ($1.12\,kg\,ha^{-1}$). The plane was a 1340 S2R Thrush flying at 110 mph (177 kph) at 10 feet (3 m) above the canopy. The spray boom was 3/4 of the wing span (38 ft or 11.6 m) with 60 nozzles delivering 7.7 gal of a pesticide and water mixture per acre ($72\,l\,ha^{-1}$) over a 45 ft (13.7 m) effective ground swath. Whirljet nozzles (ASAE Medium, size 12) (Spray Systems Co., Wheaton, IL, USA) were oriented at 180° from the direction of flight (pointing backwards). The capacity of the tank was 400 gal (1514 l) delivering the spray at 20–22 psi (138–152 kPa) (Felsot, 2002). The spraying of each field was conducted by first 'smoking' the field to determine initial prevailing wind direction. If the initial wind direction was appropriate (not blowing towards the community), the pilot would commence pesticide application by flying a series of passes perpendicular to the wind direction moving incrementally upwind. The pilot shut off pesticide flow at the end of each pass before making his turn in accordance with standard aerial application practices (Matthews, 1992).

2.3. Model selection

Two air dispersion models were considered for our modeling use. These were AgDRIFT (Stewart Agricultural Research Services, Macon, MO, USA) and the US Environmental Protection Agency's Fugitive Dust Model (FDM). AgDRIFT is a Lagrangian type spray drift model developed by the Spray Drift Task Force (a consortium of agricultural chemical companies) in collaboration with US EPA (Teske et al., 2002) as a regulatory tool to efficiently fulfill EPA's spray drift data requirements for pesticide registration in the United States. However, the AgDRIFT model interface is not amenable to modeling an actual spray event where there is changing meteorology, a moving source, and the need for user-defined receptor locations. We chose the Gaussian dispersion FDM model because of its flexibility in defining changing meteorological, source, and size distribution input parameters. Furthermore, FDM output can provide time-resolved concentration measures at user-defined receptor locations for a particular spray event. The main perceived drawback of using FDM was its inability to model evaporation; however, because our calibrated model will be used for retrospective reconstruction of exposure, and not predictively, we feel that the lack of evaporative modeling will be mostly compensated for in the calibration process.

2.4. FDM inputs

The inputs used by FDM can be divided into three categories: meteorology, source, and aerosol size distribution. The output is defined by a set of receptor locations. Two of the above three input categories are quite well characterized: meteorology and source. The least well-characterized input is the size distribution of the aerosol. The following is a brief description of how we defined the inputs and outputs. Specific details about using FDM can be found in Winges (1992).

2.4.1. Meteorology

The basic meteorological data from the day of the spray event were downloaded from the Washington State University Public Agricultural Weather System (PAWS) network (http://frost.prosser.wsu.edu/paws/About). The specific weather station where the data were collected is located 2 km south of the site over flat land. The weather information was provided in 15-min averages; among the many variables provided, we used wind speed, wind direction, and temperature.

Three other meteorological inputs used in FDM that were not provided by the PAWS network were estimated. These inputs are: surface roughness (a proxy for both the topography of the area and the type of vegetation and built structures in the area), stability class, and mixing height. Surface roughness was determined to be 5 cm from a chart based on Stull (1988) that is provided in the FDM manual (Winges, 1992). Stability class was estimated using Turner's method (Turner, 1970). According to this method, stability class ($1 = A, 2 = B, \ldots$) is a function of net radiation from solar attitude (angle of the sun determined from the Smithsonian Meteorological Tables (List, 1971)), total cloud cover, and wind speed. The boundary layer height or mixing height was determined using observations of mixing height collected by radiosonde in Boise, Idaho (Ferguson, 1998). These observations provided us with the most recent publicly available minimum and maximum mixing heights for the region. These mixing heights were comparable with mixing heights calculated from earlier (1990–1991) but geographically closer data from Spokane, WA (http://www.webmet.com/State_pages/met_wa.htm). To determine the evolution of the boundary layer height over the course of the day, we followed a profile of the mixing height over time modeled by Schichtel and Husar (2003).

During the relevant spray period, the wind speed at 10 m ranged from 1.0 to $3.6\,m\,s^{-1}$. According to the spray guidelines, $1.0\,m\,s^{-1}$ is below the minimum of $1.3\,m\,s^{-1}$; however, this low wind condition existed only during the first time period when the source was directly downwind of the community. The temperature at 1.6 m was between 21 °C and 31 °C. The relative humidity ranged from 47% to 77%. The stability class went from

stable (the first 45 min of the spray) to moderately unstable over the course of the spray. The mixing height started at around 300 m and reached 2100 m.

2.4.2. Source

The quantity of pesticide mixture sprayed was determined from information provided in Section 2.2. Emission sources in FDM are defined as either point, line, or area sources. The best approximation for an aerial application in FDM were area sources at a height of three meters above ground (the approximate pesticide release height). The emission rate was calculated from the knowledge that 7.7 gal of pesticide mixture was applied per acre over a field of known area in a known amount of time ($\approx 1.5\,\text{acre}\,\text{min}^{-1}$). This emission rate was calculated to be $2\,\text{mg}\,\text{m}^{-2}\,\text{s}^{-1}$. To interpret the model output in terms of active ingredient, we used the knowledge that a gallon of unit density liquid (water) weighs 8.32 lbs; therefore, the concentration of active ingredient of the applied pesticide mixture is 1.56% (1 lb *active* ÷ (7.7 gal × 8.32 lbs per gal)). This number allowed us to estimate the component of active ingredient in the model output. The amount of active ingredient sprayed per field (crop circle) was approximately 40 kg.

The source layout for each of the five crop circles was reconstructed from observations of the pesticide applications (Elgethun, 2004), a knowledge of the standard spraying practices, and the wind direction. The five fields in Fig. 1 were sprayed in the following clockwise order: SW, W, N, E, and S field. Based on the available 15-min meteorological data and the one hour spraying time per field, we divided each of the five fields into four equivalent areas. Each patch was then modeled as a particle emission area source at the release height of three meters during its 15-min period of pesticide application. These patches are indicated in Fig. 1 by the letters A through T, and were sprayed sequentially in that order. The first four fields were sprayed from 5:30am to 9:30am; the fifth field was sprayed from 2pm to 3pm.

2.4.3. Size distribution

Aerosol size distribution is a critical parameter influencing drift (Matthews, 1992; Teske et al., 1998). A starting point in determining a likely size distribution of the aerosol is the nozzle type used to spray the pesticide. In our study, *Whirljet* nozzles (ASAE Medium, size 12, Spray Systems Co., Wheaton, IL, USA) oriented 180° from the direction of flight (facing backward) were used (Felsot, 2002). We assumed that the aerosol size distribution is lognormal. The specification for a 'medium' spray is a lognormal distribution with a median diameter of approximately 350 μm and 1.6 geometric standard deviation (GSD). The range for what is considered a 'medium' spray according to the ASAE standard S572 is any size distribution having a volume median diameter ranging from 281 to 429 μm (ASAE, 2000). An additional complication with a liquid pesticide aerosol is that the size distribution may change as a result of evaporation. Evaporation is a function of temperature, relative humidity, mixture composition, and the original size distribution. However, FDM is limited by its inability to account for evaporation as it is a fugitive *dust* model. Nevertheless, we are confident that, although the model does not account for evaporation, through the calibration process, we can determine an *equivalent* aerodynamic size distribution that would function well for the local area. This *equivalent* size distribution is not necessarily the actual size distribution at any moment during the entire spraying event; instead it should be thought of as a size distribution that best characterizes the deposition over the entire spray period. A calculation of the evaporation time scale for a particle diameter of 300 μm, under the observed temperature and relative humidity conditions and assuming a rate of evaporation similar to water, indicated the time scale to be around half a minute (Teske et al., 2002). As the settling velocity of a 300 μm particle is approximately $1.2\,\text{m}\,\text{s}^{-1}$ (Hinds, 1999), it would take approximately 3 s for such a particle to fall 3 m (the height of pesticide release). The order of magnitude difference between settling time and evaporation time scale indicates that there is limited evaporation before deposition. Furthermore, the particle diameter changes at a relatively slow rate of $5\,\mu\text{m}\,\text{s}^{-1}$ given its initial size.

2.4.4. FDM output

The output of FDM is defined by receptor locations. Receptor locations are three-dimensional point locations defined in the community area for which air and deposition concentrations are calculated. Using FDM, we can define up to 500 points for any single model run. To obtain model output for more points, additional model runs with other receptor locations would be necessary. For our purposes, we have found that the 500 point limit is adequate for both creating a 21 by 21 point grid with a resolution of 40 m and matching model output to the 22 deposition sampler locations. The area defined by the grid is therefore 800 by 800 m.

3. Results

3.1. Model calibration by size distribution selection

With all the other inputs of the FDM model defined, the size distribution was adjusted to calibrate it. As mentioned previously, a lognormal distribution is assumed; therefore, as a lognormal distribution is described by two parameters (median diameter and geometric standard deviation (GSD)), we have a two-dimensional

parameter space to consider. For a 'realistic' size distribution, the parameter space of these two variables ranged from 10 to 600 μm for the median diameter, and 1.0 to 5.5 for the geometric standard deviation. A number of lognormal distributions, regularly spaced over this domain, was entered into FDM and the model output was compared to the actual residue measurements. Two measures of goodness of fit were considered: minimum absolute relative bias and least sum-of-squared errors (Hanna, 1988; Brusasca et al., 1989).

Relative bias (RB) is the absolute value of the relative difference between a predicted and measured value compared to the measured value. It can be expressed as follows:

$$\mathrm{RB} = \sum_{i=1}^{n} \frac{ABS(predicted_i - measured_i)}{measured_i}. \quad (1)$$

Sum-of-squared error is a classical least-squares fitting criteria and is defined as

$$\mathrm{SSE} = \sum_{i=1}^{n} (predicted_i - measured_i)^2. \quad (2)$$

The calibration process consisted of comparing deposition model results for each of 160 size distributions to the actual deposition results collected in 22 different locations within the community. Of the two goodness of fit measures, the minimum RB method was chosen over the SSE approach as the former measure weights the data more evenly; whereas, the latter places greater weight on larger differences. In our case, due to the broad range of differences, the SSE method practically allowed a single sampler to determine the model calibration. Fig. 2 shows the relative goodness of fit of the 160 different size distributions according to the RB measure. This two dimensional graph plots the parameter space of median diameter (10−600 μm) and GSD (1.0–5.5). The minimum RB occurs in the region of darkest blue; however, as there are several deep blue valleys that converge into the area located around 250−350 μm and 1.5–2.5 GSD, we examined the individual RB measures of the relevant size distributions. From this examination, we selected a lognormal size distribution of 325 μm median diameter and 2.0 GSD (marked with an 'X' on Fig. 2). There were two other size distributions where the RB measures were slightly lower; however, as those size distributions both had a median diameter of 500 μm (GSDs of 4.0 and 4.5), they were unrealistic as the nozzles used would not create such a large aerosol.

Fig. 3a shows a scatterplot of the FDM predicted deposition from the selected size distribution (325 μm, 2.0 GSD) versus the 22 actual deposition measurements. Considering the wide spread of the data, both axes are scaled logarithmically and fitted with a power law. Nearly all the predicted model data are within one

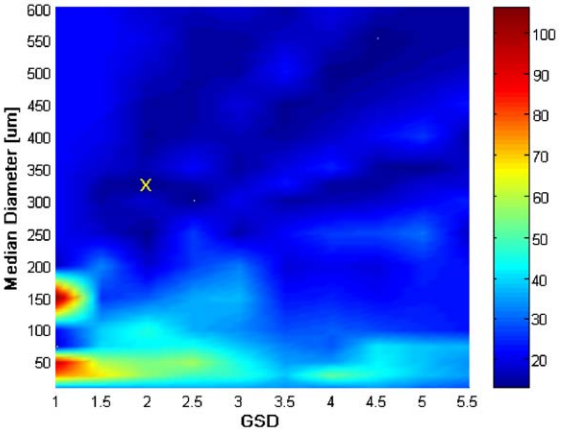

Fig. 2. Size distribution selection by the minimum RB goodness of fit measure. The median diameters ranged from 10−600 μm; the geometric standard deviation ranged from 1.0 to 5.5. The better fitting size distributions exist where the colors are a deep blue indicating that the RB is approaching a minimum. The 'X' indicates our selected size distribution for model calibration (325 μm, 2.0 GSD).

magnitude of the actual data. From the power law fit, we see that the model accounted for around 70% of the variance of the data. An examination of Fig. 3a shows that the trendline is strongly influenced by two points. These points are samplers 11 & 22, which are located right on the edge of the sprayed crop circles '*N*' and '*E*', respectively. We chose to include them because they are points where we expected large relevant deposition quantities. Spearman's non-parametric rank correlation method was also used to determine the significance of the correlation between the calibrated model output and the actual measured data (Fig. 3b). When the results were analyzed by Spearman's rank correlation, the relationship was significant with a $p<0.005$ (Fisher and vanBelle, 1993).

Table 1 shows RB, Pearson R^2, and Spearman R_s for a selection of size distributions surrounding the chosen distribution (325 μm, 2.0 GSD). Although the maximum Pearson R^2 lies at 300 μm & 2.5 GSD, we chose our size distribution according to the minimum RB and maximum Spearman R_s which coincided at 325 μm & 2.0 GSD.

3.2. Total deposition

With our model calibrated to the measured residues on the deposition samplers, we can estimate the deposition within the community by defining receptor points in a grid-like pattern over the relevant area. Total deposition is calculated by integrating deposition over the entire spray period. Total deposition is relevant for two reasons. First, the model's predicted total deposition is directly comparable with actual deposition samplers that were set out for the morning spray period.

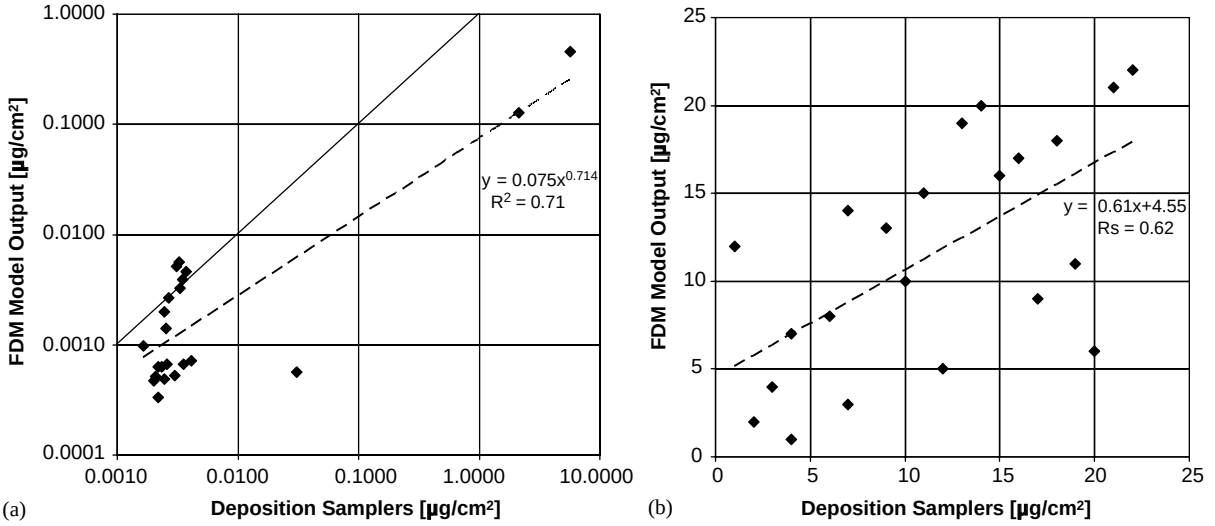

Fig. 3. Comparison of the calibrated FDM (325 μm, 2.0 GSD) deposition output and deposition sampler measurements. (a) is a scatterplot of calibrated FDM model deposition output versus deposition sampler measurements. The axes are logarithmically scaled and the data are fitted with a power-law equation. This power law explains about 70% of the data's variance. The solid line is $y = x$ line. (b) is a scatterplot comparing the ranking of calibrated FDM deposition output versus the ranking of deposition sampler measurements. The Spearman rank correlation is significant with $p < 0.005$.

Table 1
Relative bias measure and correlation coefficients for various size distributions

Size distribution	(300, 1.5)	(300, 2.0)	(300, 2.5)	(325, 1.5)	(325, 2.0)	(325, 2.5)	(350, 1.5)	(350, 2.0)	(350, 2.5)
RB	15.208	17.915	13.519	15.309	**13.455**	15.205	17.885	16.077	22.391
Pearson R^2	0.665	0.619	**0.728**	0.651	0.712	0.622	0.669	0.660	0.567
Spearman R_s	0.510	0.514	0.613	0.510	**0.616**	0.504	0.510	0.510	0.514

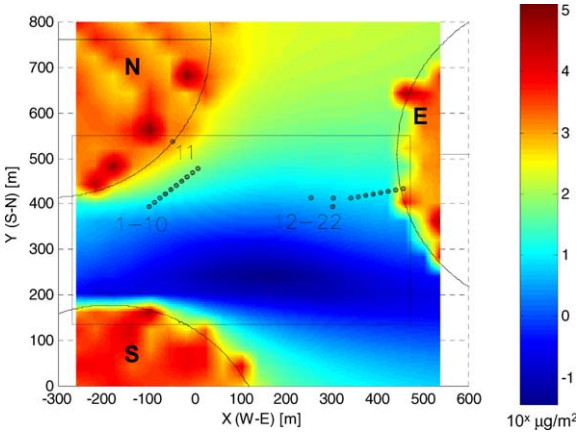

Fig. 4. Total pesticide deposition in the grid area post spray. This grid area is indicated in Fig. 1. The high concentration areas are the edges of the labeled neighboring crop circles. Concentration is plotted on a base 10 logarithmic scale. The position of the deposition samplers are indicated by the numbered dots.

Second, residents were asked to remain indoors during the morning spray period; hence, the total deposition represents the potential exposure encountered by residents upon leaving their homes. The afternoon spray of crop circle '*S*' did not contribute to deposition within the community as it was downwind. Fig. 4 is a contour map of total deposition over the larger community area. The concentration is logarithmically (base 10) scaled and the highest concentration areas correspond to the crop circles adjacent to the residences. Large portions of the community area have pesticide residue concentrations greater than $10\,\mu g\,m^{-2}$. Northern areas show total depositions greater than $100\,\mu g\,m^{-2}$.

4. Discussion

4.1. FDM model selection

FDM was selected because of the flexibility of its inputs and outputs for our modeling purposes. Despite

the model's inability to model evaporation, it accounted for roughly 70% of the variance in the log-transformed deposition data. In terms of rank correlation (the ordering of the model predictions compared with the ordering of the actual deposition loading measurements), the rank correlation was found to be significant at $p<0.005$. This result is consistent with theory as the largest size fraction of the aerosol distribution contributes most to the mass deposition and is also the slowest fraction to evaporate. Furthermore, most of the deposition is likely to have occurred rather quickly, perhaps a third of a minute or less after the spray release, leaving little time for evaporation. For example, a 100 μm unit density sphere with a settling velocity of around 0.25 m s^{-1} (Hinds, 1999), would take approximately 12 s to reach the ground from a release height of 3 m. This is further corroborated by the model calibration in which the final size distribution (325 μm and 2.0 GSD) was very close to the size distribution of the medium spray nozzle used (as specified by ASAE). Additionally, for our selected size distribution, approximately 95% of the initial mass lies in particles whose median diameters are greater than 100 μm.

A weakness of model calibration with our particular data set arises from the sparseness of our deposition data. The location of the 22 deposition samplers within the community falls into two general areas (Fig. 1). These locations were initially chosen to provide transects in areas frequented by children. In retrospect, for better model calibration, a more dispersed deployment of samplers would enhance the predictive capability of our model. Naturally, by increasing the number of deposition samples we could also improve calibration; however, analysis costs are a limiting factor for deploying a large number of deposition plates.

4.2. Total deposition

The validity of the total deposition map (Fig. 4) is only as good as the deposition measurements available to calibrate the model. The deposition data collected in our study can be said to lie in two general locations. Fig. 1 shows the two transects marked 1–10 and 12–22 in the *grid area*. These two general areas are respectively on the western and eastern sides of the residences; hence, the model's reliability is therefore quite strong between these two general locations. From these two locations going north and south, the model's predictive capacity is weaker, as we begin to extrapolate. However, as the calibrated model will be used to determine pesticide exposure where residents spend most of their time, the location of the collected deposition measurements were adequate as this area has a high degree of overlap with the childrens's time-locations shortly after the morning spray event (Elgethun, 2004).

The total deposition map, Fig. 4, indicates amounts of methamidophos active ingredient ranging from fractions of a microgram to hundreds of micrograms per square meter within the community. It is EPA's position that "applicators must not allow pesticide spray or dust to drift from the application site and contact people, animals, and certain sensitive sites, including structures people occupy at any time…." EPA recognizes that "some *de minimus* level of drift will occur from most or all applications… (EPA, 2001)"; hence, there needs to be a quantifiable approach to considering drift and human health.

By combining the total deposition map with knowledge of the location of backyards and frontyards, playgrounds, open fields, vegetable gardens, we can already gain a greater understanding of potential exposure. Moreover, by combining the approach to drift modeling illustrated in this paper with global positioning systems (GPS) for the tracking of human subjects (Elgethun et al., 2003), we can enhance exposure assessment and better characterize the risks associated with pesticide spray drift in rural agricultural communities.

4.3. Time-resolved FDM output

FDM output is time-resolved. For each receptor point, FDM calculates the deposition rate for each time period. Having calibrated our model to a lognormal size distribution of 325 μm median diameter and a GSD of 2.0, we can look at its time-resolved output. The time resolution of the model is limited by the resolution of the available meteorological input of 15 min and by the necessity for time averaging in a Gaussian model. For clarity, in Fig. 5 we show only seven of the 22 deposition locations. The other deposition points were comparable in magnitude and timing as those shown in Fig. 5. It is particularly interesting to note that deposition occurs for all but one sampler in two time periods (end of 1st h & end of 3rd h). For deposition sampler no. 22 (located right on the edge of the '*E*' field), the third deposition event occurred when that portion of the field was sprayed. The manner in which the graph is drawn is slightly misleading since the deposition does not occur instantaneously (although it probably does occur in a relatively short amount of time) as is indicated by the vertical line, but instead occurs some time within the 15 min period on which the vertical line is drawn.

By examining the effect of changing wind direction on spray drift shown in Fig. 6, we can visually see that relevant deposition occurs when the combination of wind and source location are oriented towards the community area. Just as in Fig. 5, we can see in Fig. 6 that deposition on the majority of samplers occurs in two time periods. In the first hour, the wind changes drastically from E to SSW with deposition occurring on the samplers in the last 15 min of the hour. In the third

hour the wind changes from SSW to WSW with deposition occurring on the samplers again in the last 15 min. These two figures demonstrate the episodic nature of spray drift over the community which cannot be prevented by following the general guidelines for pesticide application. To prevent off-target deposition under variable wind conditions, the pesticide applicator must have access to continuously monitored meteorology. The parameter that is most predictive of potential deposition over a particular area is wind direction.

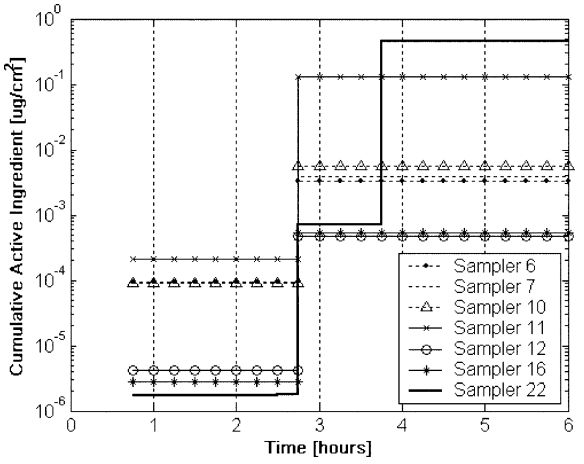

Fig. 5. FDM modeled cumulative deposition over time. The cumulative deposition of seven individual deposition samplers is plotted over time. The *y*-axis is plotted on a log scale; therefore, the initial concentration of zero is not plotted.

5. Conclusion

FDM's modeling of pesticide spray drift, using actual ground deposition measurements for model calibration, has shown that retrospective modeling of spray events can provide the necessary data for exposure assessment. Our calibrated model allowed us to account for a substantial amount of the variance in the measured deposition data. A limitation of the model was its inability to model evaporation of the aerosol; however, we have shown that the major deposition component of spray drift in our study is subject to relatively little evaporation because of the large size of the droplets and the rapidity of their settling. Nevertheless, predictions of long range drift may be subject to greater error as sampler density is lower with increasing range and evaporation effects become more significant.

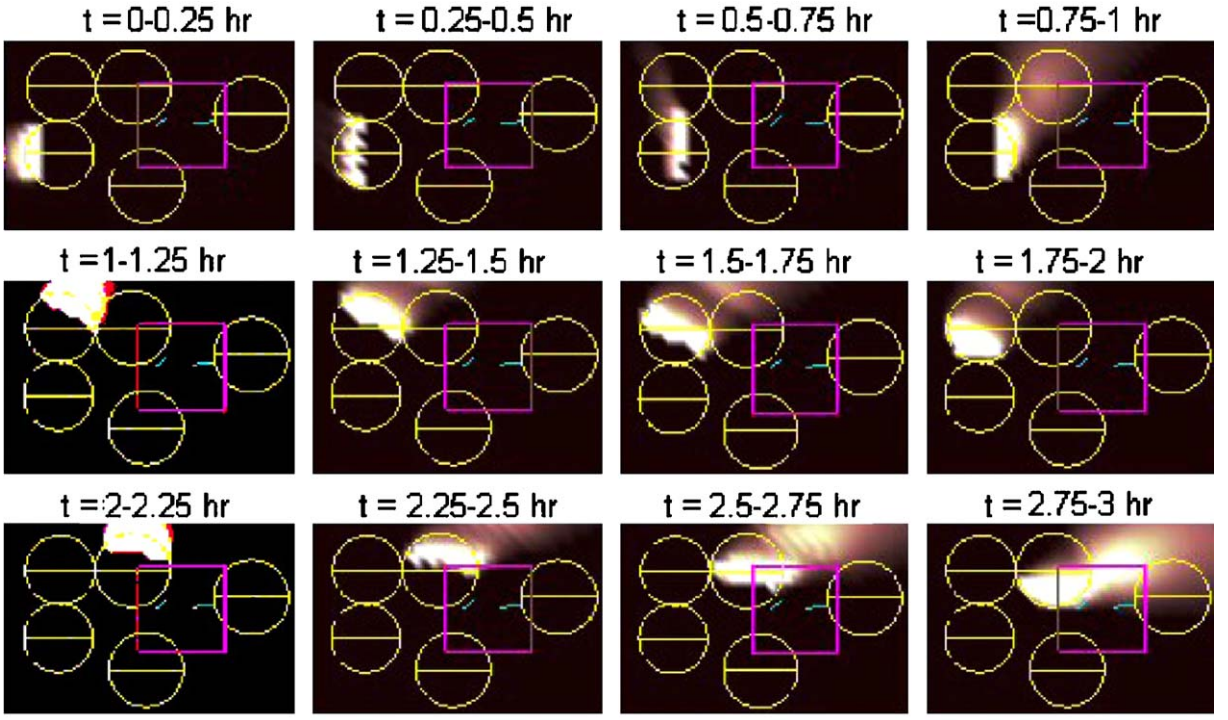

Fig. 6. FDM modeled time-sequenced drift deposition plots. Consecutive 15-min plots for the first 3 h of spraying are shown. The circles represent the sprayed fields, the square is the *grid area* and the short blue lines are the deposition sampling transects. Deposition on the majority of samplers occurs in only two time periods (end of 1st & 3rd h). The last 2 h of spraying are not shown as they do not contribute to relevant deposition as the prevailing wind direction was away from the community.

Our calibrated model also provided time-resolved concentration measurements at locations which were not sampled. Additionally, time-resolved output allowed us to gain insight into the limitations of current pesticide application guidelines with regard to changing wind direction. The perception that drift proximal to a particular community occurs relatively constantly (the assumption of general guidelines) over the duration of a spray event is strongly contradicted by our modeling which demonstrated the episodic nature of drift over a given area. Drift is clearly influenced by changing wind direction and source location in relation to the *sensitive* community area. New guidelines can be formulated to better prevent drift depending on changing meteorological conditions over the time of application. One approach would be to provide pilots with real-time local meteorological data; another related approach is to devise tolerances around meteorological parameters (i.e. wind direction) that, when exceeded, will alert the pilot to halt pesticide application.

Although our analysis was limited by the sparse distribution of our deposition samplers, the model was adequately calibrated for the purpose of community exposure assessment. In future studies an emphasis will be placed on increasing the number and spacing of deposition samplers. Having a greater spread and number of samplers would allow us to better map pesticide distribution, examine longer range drift, and conduct conditional analysis/sampling. Conditional sampling is a method by which a model can be both calibrated and validated. This would be implemented by using a portion of the measured samplers to calibrate the model, then using the remainder to validate the model predictions. Alternatively a bootstrap or jackknife analysis could be used to calibrate and validate the model using randomly selected subsets of the data.

Other improvements for future modeling would include obtaining on-site meteorological data by implementing a local weather station that would provide local wind direction, vertical wind speed and temperature profiles. Additionally, GPS tracking of the airplane or application vehicle would allow better characterization of the source term.

Acknowledgements

Special thanks to the field study staff (Sarah Weppner, Chensheng Lu, Maria Negrete, Rene Showlund) and study participants. This study was supported by the US EPA (R826886) and the National Institute of Environmental Health Sciences (PO1ES09601) Child Health Centers Program, the Agricultural Centers Program of the National Institute for Occupational Safety and Health (5 U50 OH07544), and ERC NORA training Grant (T42CCT010418).

References

Ames, R.G., Howd, R.A., Doherty, L., 1993. Community exposure to a paraquat drift. Archives of Environmental Health 48 (1), 47–52.

ASAE, 2000. ASAE Standards S572: spray nozzle classification by droplet spectra, 47th ed. American Society of Agricultural Engineers, St. Joseph, MI.

Brusasca, G., Tinarelli, G., Anfossi, D., 1989. Comparison between the results of a Monte Carlo atmospheric diffusion model and tracer experiments. Atmospheric Environment 23 (6), 1263–1280.

Elgethun, K., 2004. Global positioning system GPS tracking to characterize children's exposure to pesticides. Ph.D. Thesis, University of Washington.

Elgethun, K., Fenske, R.A., Yost, M.G., Palcisko, G.J., 2003. Time-location analysis for exposure assessment studies of children using a novel global positioning system instrument. Environmental Health Perspectives 111, 115–122.

Felsot, A.S., 2002. Interview with aerial applicator.

Fenske, R.A., Lu, C., Barr, D., Needham, L., 2002. Children's exposure to chlorpyrifos and parathion in an agricultural community in central Washington state. Environmental Health Perspectives 110 (5), 549–553.

Ferguson, S.A., 1998. Air quality climate in the Columbia River basin. General Technical Report PNW-GTR-434, U.S. Department of Agriculture, Forest Service, Pacific Northwest Research Station, Portland, Oregon.

Fisher, L.D., van Belle, G., 1993. Biostatistics: A Methodology for the Health Sciences. Wiley, New York.

Fox, R.D., Brazee, R.D., Reichard, D.L., Hall, F.R., 1990. Downwind residue from air spraying of a dwarf apple orchard. Transactions of the ASAE 33 (4), 1104–1108.

Fox, R.D., Hall, F.R., Reichard, D.L., Brazee, R.D., Krueger, H.R., 1993. Pesticide tracers for measuring orchard spray drift. Applied Engineering in Agriculture 9 (6), 501–506.

Ganzelmeier, H., Rautmann, D., Spangenberg, R., Streloke, M., Herrmann, M., Wenzelburger, H.-J., Walter, H.-F., 1995. Studies on the spray drift of plant protection products. Technical report, Federal Biological Research Centre for Agriculture and Forestry, Berlin.

Garcia, A.M., Sabater, M.C., Mendoza, M.T., Ballester, F., Carrasco, J.M., 2000. Exposure to organophosphate pesticides in a general population living in a rice growing area: an exploratory study. Bulletin of Environmental Contamination and Toxicology 65, 764–771.

Hanna, S.R., 1988. Air quality model evaluation and uncertainty. Journal of the Air Pollution Control Association 38, 406–412.

Hinds, W.C., 1999. Aerosol Technology: Properties, Behavior, and Measurement of Airborne Particles, 2nd ed. Wiley, New York.

Koch, D., Lu, C., Fisker-Andersen, J., Jolley, L., Fenske, R.A., 2002. Temporal association of children's pesticide exposure and agricultural spraying: report of a longitudinal biomonitoring study. Environmental Health Perspectives 110, 829–833.

List, R.J. (Ed.), 1971. Smithsonian Meteorological Tables. Smithsonian Miscellaneous Collections, 6th review ed. vol. 114, Smithsonian Institution, Washington.

Lu, C., Fenske, R.A., Simcox, N.J., Kalman, D., 2000. Pesticide exposure of children in an agricultural community: evidence of household proximity to farmland and take home exposure pathways. Environmental Research 84, 290–302.

MacCollom, G.B., Currier, W.W., Baumann, G.L., 1985. Pesticide drift and quantification from air and ground applications to a single orchard site. American Chemical Society Symposium Series 273, 189–199.

MacNeil, J.D., Hikichi, M., 1986. Phosmet residues in an orchard and adjacent recreational area. Journal of Environmental Science and Health B21, 375–385.

Matthews, G.A., 1992. Pesticide Application Methods, 2nd ed. Longman Scientific & Technical, Essex, England.

Pesticide Registration (PR) Notice 2001-X Draft (Spray and dust drift label statements for pesticide products) EPA—US Environmental Protection Agency, 2001, available from ⟨http://www.epa.gov/opppmsd1/PR_Notices/prdraft-spraydrift801.htm⟩.

Ramaprasad, J., Tsai, M.Y., Elgethun, K., Hebert, V.R., Felsot, A., Yost, M.G., Fenske, R.A., 2004. The Washington aerial spray drift study: assessment of off-target organophosphorus insecticide atmospheric movement by plant surface volatilization. Atmospheric Environment 38 (33), 5703–5713.

Richards, S.M., McClure, G.Y.H., Lavy, T.L., Mattice, J.D., Keller, R.J., Gandy, J., 2001. Propanil (3,4-dichloropropionanilide) particulate concentrations within and near the residences of families living adjacent to aerially sprayed rice fields. Archives of Environmental Contamination and Toxicology 41, 112–116.

Salyani, M., Cromwell, R.P., 1992. Spray drift from ground and aerial applications. Transactions of the ASAE 35 (4), 1113–1120.

Schichtel, B.A., Husar, R.B., 2003. Regional simulation of atmospheric pollutants with the CAPITA Monte Carlo model. Center for Air Pollution and Trend Analysis, available from ⟨http://capita.wustl.edu/CAPITA/CapitaReports/MonteCarlo/MonteCarlo.html⟩, 1995 [cited 7 December 2003].

Shehata, T., Richardson, E., Cotton, E., 1984. Assessment of human population exposure to carbaryl from the 1982 Maine spruce budworm spray project. Journal of Environmental Health 46, 293–296.

Stull, R.B., 1988. An Introduction to Boundary Layer Meteorology. Kluwer Academic Publishers, Boston.

Teske, M.E., Thistle, H.W., Eav, B., 1998. New ways to predict aerial spray deposition and drift. Journal of Forestry 96 (6), 25–31.

Teske, M.E., Bird, S.L., Esterly, D.M., Curbishley, T.B., Ray, S.L., Perry, S.G., 2002. Agdrift: a model for estimating near-field spray drift from aerial applications. Environmental Toxicology and Chemistry 21 (3), 659–671.

Turner, D.B., 1970. Workbook of Atmospheric Dispersion Estimates. U.S. Environmental Protection Agency, Research Triangle Park, N.C. (ap-26 Ed.).

Valent, MONITOR 4 Spray. Valent USA Corporation, Walnut Creek, CA. 2001, available from ⟨http://www.valent.com ⟩.

Weppner, S., Elgethun, K., Lu, C., Yost, M.G., Hebert, V., Fenske, R.A., 2005. The Washington aerial spray drift study: Children's exposure to methamidophos in an agricultural community following fixed-wing aircraft applications. Journal of Exposure Analysis and Environmental Epidemiology, in press.

Winges, K.D., 1992. User's Guide for the Fugitive Dust Model (FDM) (revised epa-910/9-88-202r Ed.). US Environmental Protection Agency, 1200 Sixth Avenue, Seattle, WA 98101.